Journal of Materials Chemistry C

COMMUNICATION

Improving the electrical performance of solution processed oligothiophene thin-film transistors via structural similarity blending

Received 00th January 20xx,
Accepted 00th January 20xx

DOI: 10.1039/x0xx00000x

www.rsc.org/

Tim Leydecker,[a] Laura Favaretto,[b] Duc Trong Duong,[c] Gabriella Zappalà,[d] Karl Börjesson,[a,e] Antonino Licciardello,[d] Alberto Salleo,[c] Manuela Melucci,*[b] Emanuele Orgiu*[a,f] and Paolo Samorì*[a]

Here we show that the blending of structurally similar oligothiophene molecules is an effective approach to improve field-effect mobility and I_{on}/I_{off} as compared to single components based transistors. The effect of addition of each component is studied extensively using a wide array of methods such as X-Ray diffraction, ToF-SIMS, Ambient UPS correlated with the electrical characterization.

Introduction

Blending (macro)molecules is a powerful approach to develop novel multicomponent materials with improved performances for various technological applications. Each component can also confer a well-distinct property to the ensemble, with the ultimate goal of fabricating multifunctional conjugated materials and opto-electronic devices.[1-5]

Among various examples, the most well-known cases involve the blending of fullerene derivatives with polymers for solar cell applications,[6-10] or TIPS-pentacene combined with a wide array of polymers for improving the field-effect mobility.[11-21] Less attention has been paid on investigating blends of small semiconducting molecules: a few studies were carried out that usually focused on structurally dissimilar and differently sized components such as $PC_{70}BM$ and $DTS(PTTh_2)_2$.[22, 23]

Among various families of small semiconducting molecules, oligothiophenes have attracted a great attention because of their ease of synthesis combined with their interesting charge transport characteristics.[24-29] While the formerly developed unsubstituted derivatives were processed by means of thermal sublimation,[30, 31] oligothiophenes functionalized with alkyl side-chains made solution processing possible.[32, 33] In particular, di-hexyl-substituted oligothiophenes (DHnTs) are easily accessible model *p*-type molecules that have proven to display a high environmental stability, due to their ability to self-assemble into tightly packed architectures which are exposing hexyl chains, the latter acting as a protecting layer.[34-36] When self-assembled in-between the source and drain electrodes of thin-film transistors (TFTs) it revealed efficient charge transport characteristics, as witnessed by high field-effect mobilities.[37] We have recently demonstrated that drop-cast dihexylquaterthiophene (DH4T) thin-films could exhibit electrical performances comparable to those of vacuum-sublimed layers.[38, 39] Such an outstanding result was achieved through a careful choice of the source/drain and gate dielectric surface functionalization to tune surface energies, and by controlling the kinetics of the self-assembly process via optimization of the solvent evaporation rate. Along this line, aiming at exploiting ever effective and simple approaches for further enhancing the performances of solution processed TFT, here we opt for a strategy based on the structure similarity blending (SSB). Such a strategy relies on the blending of structurally similar molecular semiconductors as active layers in TFT. Similarity blending effects on morphology and electrical performances in organic TFTs has been already investigated extensively in the case of polydisperse polymers that can be considered as a blend of similar molecules with varying contour lengths. However, such systems lack the precise control over its components, consisting of a broad range of polymers.[40, 41] In the present study we blend organic semiconducting molecules belonging to the same chemical family (i.e. dihexyl substituted oligothiophenes) but having different length of the π-conjugated backbone. Molecular blends of oligothiophene-based small molecules have already demonstrated the possibility of achieving color tunability,[42] but no electrical characterization of such systems is reported yet, to the best of our knowledge. Remarkably, by exploiting DH4T as a model compound, we demonstrate that its electrical performances, when integrated in blend in bottom-contact bottom-gate TFT devices, can be enhanced up to two

[a] *University of Strasbourg, CNRS, ISIS UMR 7006, 8 allée Gaspard Monge, F-67000 Strasbourg, France.*
[b] *CNR-ISOF, Via P. Gobetti 101, 40129 Bologna, Italy.*
[c] *Department of Materials Science and Engineering, Stanford University, Stanford, California 94305, United States.*
[d] *Dipartimento di Scienze Chimiche, Università degli studi di Catania, v.le A. Doria 6, 95125 Catania, Italy.*
[e] *Present address: Department of Chemistry and Molecular Biology, University of Gothenburg, Kemigården 4, 412 96 Göteborg, Sweden.*
[f] *Present address: Institut National de la Recherche Scientifique (INRS), EMT Center, 1650 Blvd. Lionel Boulet, J3X1S2 Varennes, Canada.*
Corresponding Authors: samori@unistra.fr , emanuele.orgiu@emt.inrs.ca , manuela.melucci@isof.cnr.it
Electronic Supplementary Information (ESI) available: [details of any supplementary information available should be included here]. See DOI: 10.1039/x0xx00000x

orders of magnitude by combining it with DH2T and DH6T molecules.

Experimental Section

Dihexylquaterthiophene (DH4T) was either purchased from Polyera under the name ActivInk P0400 or synthesized. Dihexylbithiophene (DH2T) was purchased from Sigma Aldrich. Both were used as received, without further purification. DH4T and dihexylsexithiophene (DH6T) were synthesized accordingly to an already reported procedure.[43] The solvents were purchased from Sigma-Aldrich and used without further purification. Substrates for bottom-contact bottom-gate transistors were purchased from Fraunhofer Institute. They consist of n^{++}-Si substrates with 230 nm of thermally grown SiO_2 as the gate dielectric (C_o = 15 nFcm^{-2}) and pre-patterned pairs of gold electrodes with interdigitated geometry as the source and drain. All samples were prepared and measured in a N_2-filled glovebox to avoid oxidative doping of the materials and ensure reproducibility of the experiments. Solution preparation, hexamethyldisilazane (HMDS) treatment, and electrode functionalization were performed under N_2 atmosphere. Gold electrodes functionalization consisted of their immersion into a 4 mM solution of 1-decanethiol (C_{10}) in ethanol for 12 h. The substrates were thoroughly rinsed by squirting with 100 µL of absolute ethanol five times. HMDS, which was purchased from Sigma-Aldrich, was spin-coated at 1500 rpm on the substrate and annealed for 1 h at 100 °C.

The properties of organic TFTs were evaluated under positive or negative gate bias to explore the majority charge carrier type and device performance. Experimental data were analyzed using standard TFT equations (for p-type semiconductors) in the saturation regime:

$$I_{DS} = -\frac{W}{2L}\mu C_0 (V_{GS} - V_{Th})^2$$

where I_{DS} is the source-drain current, V_{GS} is the gate voltage, C_0 is the capacitance per unit area of the dielectric layer, V_{Th} is the threshold voltage, and µ is the field-effect mobility in the saturation region. The mobilities were determined in the saturation regime at V_{DS} = −60 V from the slope of plots of $I_{GS}^{1/2}$ versus V_{GS}. In all the characterized sets, the voltage range was kept constant (40 V to -60 V) for both I_{DS}–V_{DS} and I_{DS}–V_{GS} to ensure full comparison among different samples.

An ambient photoelectron spectrometer (AC-2, by RKI Instruments) working at ambient conditions was employed to determine the ionization energy (IE) of the DHnT films and the work function of the different SAM-functionalized gold electrodes.

ToF-SIMS depth profiles were obtained by using a TOF-SIMS IV (IONTOF GmbH, Muenster). All measurements were performed in dual beam configuration, non-interlaced mode, alternating analysis cycles with sputtering cycles and detecting in positive ion mode. 20 keV C_{60}^{++} ions were used for sputtering, while a 25 keV Bi_3^+ ions were used for analysis of the central part of the crater produced by the sputter beam. In order to minimize the sample damage induced by the bismuth primary beam, in all measurements the C_{60}-to-Bi dose ratio was kept larger than 5x10^2.

A JASCO V-630 spectrophotometer was employed to record the absorbance spectra of DH4T dissolved in dichlorobenzene and of drop-casted films of DH4T containing small amounts of DH2T.

Results and discussion

In order to improve the electrical characteristics of thin-films based on DH4T, we have combined such molecule with other di-hexyl-substituted oligothiophenes (DHnT) analogues.[37] Such analogues exhibit either two or six thiophenes in the main conjugated backbone for DH2T or DH6T, respectively (**Figure 1**). While the hexyl side chains guarantee good solubility in common organic solvents, the presence of oligothiophene backbones with variable lengths is known to determine the optical and electrical characteristics of the material.[44-46] Through the controlled blending of DH4T we aim at unravelling and exploiting three possible structural/morphological effects. First, when combined with shorter oligomers like DH2T one could expect to have the latter component filling the grain boundaries of the DH4T crystalline assembly. Second, when mixed with a longer and less soluble DH6T oligomer, one may expect the latter to act as seed of crystallization of DH4T or at least to undergo crystallization more quickly. Third, the variation of the oligothiophene length could be accompanied with a vertical phase segregation within the film which could also affect drastically the TFT performance in bottom-gate bottom-contact devices.

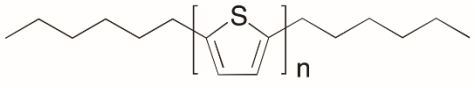

Figure 1. Molecular structure of DHnT molecules. The studied molecules contained a various number of thiophene units: n=2 (dihexylbithiophene, DH2T), n=4 (dihexylquaterthiophene, DH4T) and n=6 (dihexylsexithiophene, DH6T).

Table 1. Correlation between solvent and electrical performances of pristine DH4T TFTs. All films were drop-cast on HMDS-treated SiO_2 and untreated Au electrodes.

Solvent	Average field-effect mobility [cm²/Vs][a]	I_{on}/I_{off}
Chloroform	3.4±1.1 ×10^{-5}	10^1-10^4
Chlorobenzene	1.1±0.7 ×10^{-3}	10^1-10^4
Dichlorobenzene	6.6±4.3 ×10^{-3}	10^4-10^6
Dichlorobenzene (optimized procedure)	3.1±1.2 ×10^{-2}	10^4-10^5

[a] Averaged over 16 tested devices

We started by fabricating pristine DH4T-based transistors by making use of the previously reported optimized procedure which relies on the use of HMDS treatment of the dielectric SiO_2 surface and a processing using a slow evaporating solvent like dichlorobenzene (DCB) (**Table 1**). The sample was kept in a sealed environment after deposition in order to reduce the evaporation rate. The analysis of the other DHnT based pristine devices revealed that when DH2T is deposited as single component thin film, it displays no measurable charge transport characteristics once integrated in a transistor. Not surprisingly, the addition of even small amounts of DH2T to DH4T containing devices resulted in a strong decrease in field-effect mobility (**Figure 2**). At 4 wt% of DH2T

present in the blend, the measured mobilities were very low (mobilities of 2 ×10^{-4} cm²/Vs with I_{on}/I_{off} around 10^3 over 4 working devices). This can be explained by (i) DH2T disrupting the structural features of the DH4T films, (ii) DH2T acting as a trap for charges within the channel, and/or (iii) DH2T forming a thin layer at the interface with the dielectric, where most of the charges are transported in a bottom-contact bottom-gate transistor.[47]

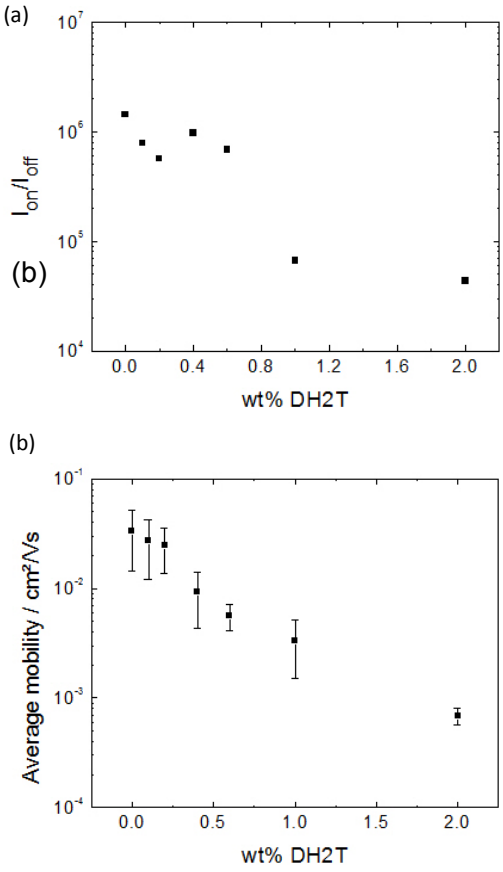

Figure 2. Electrical performances as a function of the amount of DH2T added to DH4T (optimized procedure using HMDS and DCB at slow evaporation rate). Both the values of (a) the I_{on}/I_{off} and (b) the field-effect mobility as a function of wt% DH2T were obtained from transfer curves (average over 8 transistors with L = 2.5 µm; 5 µm; 10 µm; 20 µm).

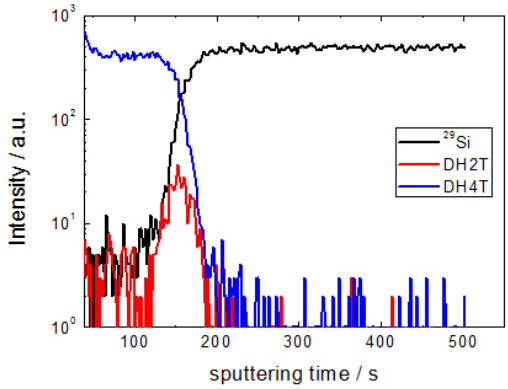

Figure 3. ToF-SIMS on bare Si, of a film resulting from a drop-cast of a DH4T/DH2T blend in dichlorobenzene. (2% wt DH2T)

Grazing Incident X-Ray Diffraction (GIXD) measurements were carried out on pristine DH4T films and those blended with DH2T as deposited from a dichlorobenzene solution. The results revealed that the addition of small amounts of DH2T into the DH4T solution does not significantly alter the crystalline nature of DH4T films (**Figure S1**). This conclusion is further supported by UV-Vis spectroscopy. The absorbance spectra of pure DH4T in solution in DCB and in solid film are markedly different (**Figure S2**). In solution, a single absorption peak centered at 409 nm is observed. Films of DH4T show a more structured spectrum, with a large absorption peak at higher energies, and a smaller one at lower energies. When analyzing the absorbance spectra of the solid film within the framework of the exciton model,[48] the two new peaks arising in the film indicate that DH4T is crystalizing in a parallel rather than a slip stacked arrangement, in accordance with the published crystal structure.[36] Furthermore, the addition of small amounts of DH2T into the films does not change the shape of the absorption spectra, concurring with the conclusion from the GIXD measurements that the crystalline nature of DH4T is unaltered by the addition of small amounts of DH2T. These findings rule out option (i). Photoelectron spectroscopy in air (PESA) measurements were performed to determine the Ionization Energy (IE) of the molecules. A large difference between DH2T and DH4T was measured, with values of 5.98 eV and 5.2 eV, respectively. Such a difference reveals highly unfavorable charge transfer from DH4T into DH2T, ruling out option (ii) as well. Therefore, the localization along the Z-axis of the DH2T within the blend film was investigated by means of Time of Flight Secondary Ion Mass Spectrometry (ToF-SIMS) measurements. These measurements were performed by using a fullerene beam as sputter erosion of the sample since it is known to allow "molecular depth profiling" of many organic systems while minimizing the ion-induced damage usually observed when using monoatomic ions.[49] In our experiments depth profiles were obtained by alternating sputtering cycles with the C_{60} beam with the analysis of the crater bottom accomplished by using a very low current Bi_3^+ beam. The latter produces, without introduction of appreciable damage in the sample ("static SIMS" conditions),[50] the secondary ions that are mass analyzed in the time-of-flight spectrometer. The molecular depth profile (**Figure 3**) shows the evolution of the protonated molecular ions of DH4T (m/z 499) and DH2T (m/z 335) as function of sputtering time, that can be assumed to be proportional to depth. The profile shows a clear accumulation of the lower molecular weight component (DH2T) in the interfacial region with silicon, with the top of the film consisting essentially of pure DH4T. In other words, the film is enriched in DH2T at the semiconductor-dielectric interface, where most of the charges flow between the source and the drain electrode, confirming scenario (iii). The very slow evaporation of the solvent in the optimized procedure is providing enough time for the DH2T and DH4T to undergo phase segregation. Therefore, the same blend was produced, using either dichlorobenzene or chloroform as the solvent, without modification of the evaporation rate as done in the optimized procedure through the self-assembly in an atmosphere saturated by the vapors of a given solvent.

The electrical performances of samples produced from DH4T/DH2T blends in chloroform and DCB (without reduction of the evaporation rate) were tested. The field-effect mobilities with the increasing DH2T content within the films are reported in **Figure 4**. A small increase of the mobilities at low quantities of DH2T was observed in both cases. The mobilities of devices produced from DCB (normal evaporation rate) were greater than those measured

in devices produced from $CHCl_3$. Unfortunately, the increase in electrical performance is rather modest, which can easily be explained by the insulating nature of DH2T, due to a very wide band gap of 3.6 eV (as compared to 2.6 and 2.8 for DH6T and DH4T, respectively), as reported by Facchetti et al.[51] With the increasing amount of DH2T, the performance of the devices appears more and more modest.

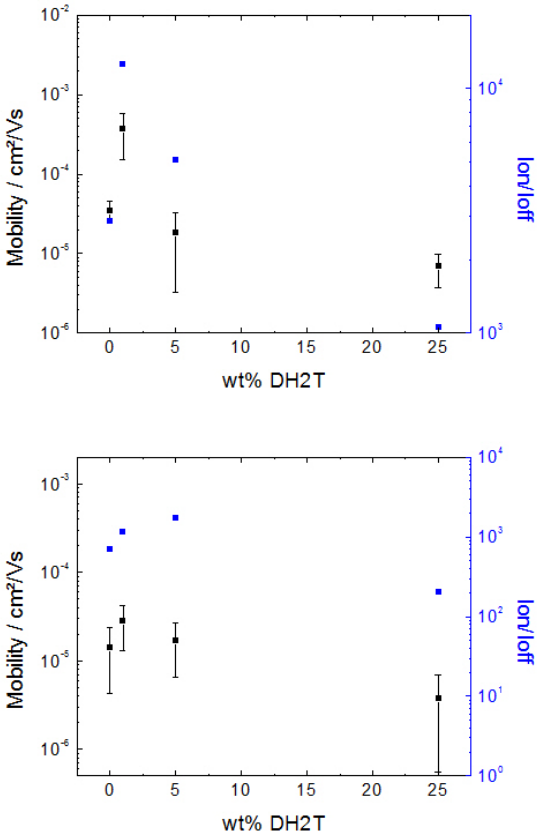

Figure 4. Field-effect mobilities and I_{on}/I_{off} as a function of the amount of DH2T added to DH4T. Mobilities and I_{on}/I_{off} of films deposited from (a) dichlorobenzene at high evaporation rate, and (b) chloroform. The mobility as a function of wt% DH2T were obtained from transfer curves (average over 8 transistors with L = 2.5 µm; 5 µm; 10 µm; 20 µm).

In view of the lack of improvement in the electrical characteristic of DH4T when blended with DH2T, we have focussed our attention to the combination of DH4T with DH6T, with a particular attention to the effect of blending on the electrical characteristics of DH4T. Towards this end, different amounts of DH6T were added to DH4T in a chloroform solution. Electrical characteristics of devices obtained by depositing these solution onto bottom-gate bottom contact TFTs are reported in **Figure 5**. While mobilities of devices based on pristine components differ only of one order of magnitude (μ_{DH4T} = 3.4 × 10^{-5} cm²/Vs; μ_{DH6T} = 4.6 × 10^{-6} cm²/Vs), the I_{on}/I_{off} such pristine films differ of as many as 4 orders of magnitude, with DH6T exhibiting a very poor semiconducting characteristics characterized by an I_{on}/I_{off} as low as 20. Significantly, an impressive improvement of charge-transport characteristics has been observed when using a blend with an excess of DH6T, i.e. DH4T:DH6T=10%:90%, quantified by a 50-fold and 300-fold increase in mobility compared to the pristine DH4T and DH6T, respectively. In terms of I_{on}/I_{off}, the most favorable blend was obtained by using equal amounts of each component (I_{on}/I_{off} = 5 × 10^5), being 4 orders of magnitude greater than for the neat DH6T, with values rather close to those of DH4T both in terms of mobility and I_{on}/I_{off}. I_{DS}-V_{GS} curves are presented in **Figure 5**, output curves are reported in **Figure S4**, V_{Th} and I_{off} as a function of DH6T wt% are reported in **Figure S5**. We observe that both in terms of current range and shape of transfer curves, the samples containing from 100% to 50% of DH4T exhibit very similar transfer curves, demonstrating a very minor effect of the DH6T on the charge transport mechanism in the channel of the device. Optical microscope images (**Figure S7**) reveal that most of the DH6T present in the channel forms aggregates that are not large enough to bridge the channel, explaining the minor impact on the measured electrical performances. However, output curves indicate progressive reduction of the contact resistance with increased amounts of DH6T in the blend. This is explained by the gold-semiconductor interface since the HOMO level of DH6T is lower compared to that of DH4T.

a)

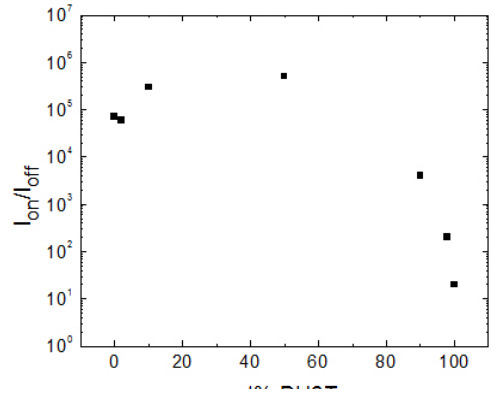

(b)

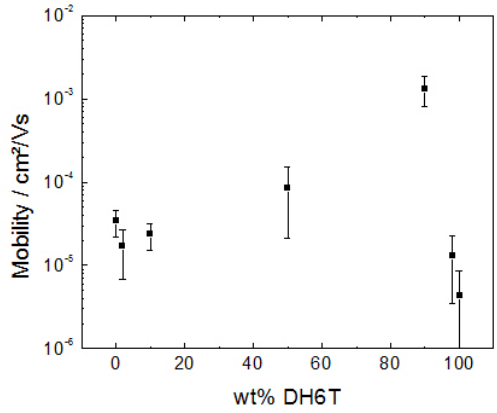

(c)

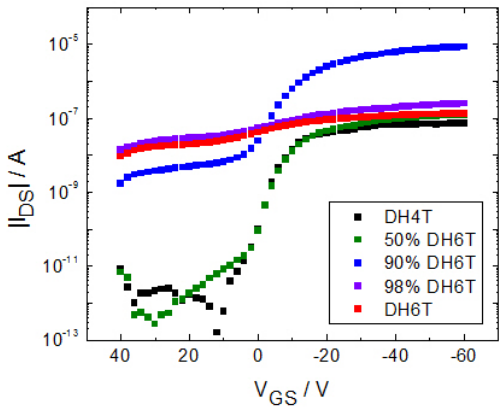

Figure 5. Electrical characteristics as a function of the amount of DH6T added to DH4T. Both the values of (a) the I_{on}/I_{off} and (b) the field-effect mobility as a function of wt% DH6T were obtained from transfer curves (average over 8 transistors with L = 2.5 µm; 5 µm; 10 µm; 20 µm). (c) Transfer curves of transistors with different amounts of DH4T and DH6T (L = 20 µm).

On the other hand, when the film contains an excess of DH6T, even small amounts of DH4T (5-10%) result in major changes in mobility, I_{on}/I_{off} and threshold voltage. Interestingly, the films made from a 10% DH4T-90% DH6T exhibit characteristics that are peculiar to both materials, i.e. a high (DH6T-like) off current and a low (DH4T-like) threshold voltage. However, the two features stem from different portions of the film along Z. In particular, the parasitic low-resistive contributions that determine the I_{off} are usually directly proportional to the film thickness and stem from the top portions of the film. Conversely, the threshold voltage is generally dominated by interfacial traps located either at the semiconductor-dielectric or semiconductor-electrodic interface. A DH6T-like bulk is not surprising in a film comprising 10% DH4T-90% DH6T since the latter accounts for most of the film volume. The observed increases in electrical performances at this ratio are very interesting since the highest observed mobilities would be expected to be at best equal to the mobilities of either DH4T or DH6T, if the materials were completely phase-segregated. While the high I_{on}/I_{off} could be explained by DH6T aggregates surrounded by DH4T areas, the observed mobility is likely due to a complete change in crystallinity of either DH4T, DH6T or both upon blending.

By and large, charge transport in DHnT blends can be strongly affected by the addition of a small quantity of another (similar) oligothiophene. While very small amounts of DH6T added to the smaller molecule DH4T determine a decrease in charge transport, the opposite scenario (small amounts of DH4T added to the DH6T solution) results in a drop in the mobility of the devices, similarly to the case of DH2T/DH4T pair, but with a largely superior 30-fold improvement upon addition of the smaller oligothiophene (comparison of mobilities provided in **Figure S6**). This can be explained either by the structural characteristics of the blended film (in particular, phase segregation), or by DH6T acting as a trap for charges.

In order to cast light onto the first hypothesis, PESA measurements were carried out. With a penetration depth below 4 nm, PESA measurements provide precious information on the composition of the film at the top surface. It revealed that the Ionization Energy (IE) of DH4T is markedly different from that of DH6T, amounting to 5.2 eV and 4.85 eV, respectively. The values of the Ionization Energy as a function of the amount of each material in the blend are reported in **Figure S8**. The IE was found to be constant for blends ranging from pure DH4T to 50:50 DH4T:DH6T blends, indicating that at such ratio DH4T forms a film over the DH6T. This can be explained by the lower solubility of DH6T, leading to the sudden formation of DH6T aggregates, that are present in the bottom of the film upon solvent evaporation. Unfortunately, because of the high roughness in DH6T films deposited from a chloroform solution, TOF-SIMS measurements did not provide reproducible results. The fact that the DH6T lies at the interface between the SiO_2 dielectric surface and DH4T explains the observed drop in mobility for small percentages of DH6T reported in **Figure 4**. Since the IE of DH6T is lower than that of DH4T, charges get trapped in the DH6T at the interface. At small quantities of DH4T, the large error bars are due to the disparity on the x/y-scale of the layer within each tested sample. Nevertheless, the DH4T seem to affect the observed IE even when present in small quantities, due to its position over the DH6T. The observed improvement in electrical characteristics can be likely attributed to the effect of DH4T bridging the DH6T crystallites leading to better percolation paths connecting source and drain electrodes. Furthermore, these areas of DH4T separating DH6T are sufficient to inhibit charge transport when I_{DS} is below $V_{Th,DH4T}$. These observations unambiguously show how effective is our method of blending two similar materials with different physico-chemical properties in order to improve their electrical characteristics. This approach can be surely applied to other classes of materials and for improving or controlling other type of properties.

Conclusions

In summary, we have demonstrated that by blending structurally similar oligothiophenes using a low-boiling point solvent such as chloroform, the field-effect mobility of DH4T could be improved by two orders of magnitude. Such an enhancement is achieved by simple combining it with another similar-performing small molecule from the same family (DH6T). The addition of very small quantities of a less synthetically expensive and non-semiconducting molecule (DH2T) was proven to be an effective way of affecting the electrical performance of the tested transistors. When a high boiling point solvent was used, phase segregation along the z-axis was observed, reducing electrical performances. On the other hand, the use of a low boiling point solvent such as chloroform (hindering the thermodynamically favored phase segregation in multicomponent films) led to an improvement of performances in the bi-component blend, similarly to DH6T/DH4T blends. While most methods relying on multiple semiconducting materials in the same devices focus on separate layers, with multiple processing difficulties, our approach of blending proved to be simple, effective and can be adapted to most semiconducting small molecules for improved processability and performances. This approach would open new perspectives in the tuning of electrical performances of TFT by appropriate doping the semiconducting layer. Moreover, our processing method, based on drop-casting, a technique similar to ink-jet printing, as a means to achieve high mobility devices is compatible with large-area applications thus providing a pathway towards organic electronics that satisfies the needed balance between performance and processability. In each case, study of the electrical characteristic of the bi-component blends in a bottom-gate bottom-contact TFT was crucial to gain insight into the structure film at the bottom interface, while the top surface was probed by ionization energy measurements. This innovative and simple approach to film-structure determination can substitute more traditional techniques such as AFM and ToF-SIMS, as it allows strong discrimination between molecules that differ by their electrical characteristics and energy levels.

Acknowledgements

We thank Prof. Dr. Klaus Müllen for enlightening discussions on phase segregation in multicomponent transistors. This work was financially supported by EC through the ERC project SUPRAFUNCTION (GA-257305) and the Marie Curie ITN project iSwitch (GA No. 642196), the ANR Labex project CSC (ANR-10-LABX-0026 CSC) within the Investissement d'Avenir program ANR-10-IDEX-0002-02, and the International Center for Frontier Research in Chemistry (icFRC).

Keywords: oligothiophenes • OTFT • semiconductor blends • phase segregation • drop-casting

Notes and references

1. K. Asadi, D. M. De Leeuw, B. De Boer and P. W. M. Blom, *Nat. Mater.*, 2008, **7**, 547-550.
2. H. X. Shang, H. J. Fan, Y. Liu, W. P. Hu, Y. F. Li and X. W. Zhan, *Adv. Mater.*, 2011, **23**, 1554-1557.
3. M. Y. Li, N. Stingelin, J. J. Michels, M. J. Spijkman, K. Asadi, R. Beerends, F. Biscarini, P. W. M. Blom and D. M. de Leeuw, *Adv. Funct. Mater.*, 2012, **22**, 2750-2757.
4. E. Orgiu, N. Crivillers, M. Herder, L. Grubert, M. Patzel, J. Frisch, E. Pavlica, D. T. Duong, G. Bratina, A. Salleo, N. Koch, S. Hecht and P. Samorì, *Nat. Chem.*, 2012, **4**, 675-679.
5. E. Orgiu and P. Samorì, *Adv. Mater.*, 2014, **26**, 1827-1845.
6. M. Reyes-Reyes, K. Kim and D. L. Carroll, *Appl. Phys. Lett.*, 2005, **87**.
7. X. N. Yang, J. Loos, S. C. Veenstra, W. J. H. Verhees, M. M. Wienk, J. M. Kroon, M. A. J. Michels and R. A. J. Janssen, *Nano. Lett.*, 2005, **5**, 579-583.
8. Y. Kim, S. Cook, S. M. Tuladhar, S. A. Choulis, J. Nelson, J. R. Durrant, D. D. C. Bradley, M. Giles, I. McCulloch, C. S. Ha and M. Ree, *Nat. Mater.*, 2006, **5**, 197-203.
9. H. C. Hesse, J. Weickert, C. Hundschell, X. L. Feng, K. Müllen, B. Nickel, A. J. Mozer and L. Schmidt-Mende, *Adv. Energy Mater.*, 2011, **1**, 861-869.
10. W. C. Chen, Z. K. Du, M. J. Xiao, J. Zhang, C. P. Yang, L. L. Han, X. C. Bao and R. Q. Yang, *ACS Appl. Mater. Inter.*, 2015, **7**, 23190-23196.
11. D. M. Russell, C. J. Newsome, S. P. Li, T. Kugler, M. Ishida and T. Shimoda, *Appl. Phys. Lett.*, 2005, **87**.
12. J. Kang, N. Shin, D. Y. Jang, V. M. Prabhu and D. Y. Yoon, *J. Am. Chem. Soc.*, 2008, **130**, 12273-12275.
13. R. Dabirian, V. Palermo, A. Liscio, E. Schwartz, M. B. J. Otten, C. E. Finlayson, E. Treossi, R. H. Friend, G. Calestani, K. Müllen, R. J. M. Nolte, A. E. Rowan and P. Samorì, *J. Am. Chem. Soc.*, 2009, **131**, 7055-7063.
14. R. Hamilton, J. Smith, S. Ogier, M. Heeney, J. E. Anthony, I. McCulloch, J. Veres, D. D. C. Bradley and T. D. Anthopoulos, *Adv. Mater.*, 2009, **21**, 1166-1171.
15. D. K. Hwang, C. Fuentes-Hernandez, J. B. Kim, W. J. Potscavage and B. Kippelen, *Org. Electron.*, 2011, **12**, 1108-1113.
16. A. Liscio, G. P. Veronese, E. Treossi, F. Suriano, F. Rossella, V. Bellani, R. Rizzoli, P. Samorì and V. Palermo, *J. Mater. Chem.*, 2011, **21**, 2924-2931.
17. E. Orgiu, A. M. Masillamani, J. O. Vogel, E. Treossi, A. Kiersnowski, M. Kastler, W. Pisula, F. Dötz, V. Palermo and P. Samorì, *Chem. Commun.*, 2012, **48**, 1562-1564.
18. J. Smith, W. M. Zhang, R. Sougrat, K. Zhao, R. P. Li, D. K. Cha, A. Amassian, M. Heeney, I. McCulloch and T. D. Anthopoulos, *Adv. Mater.*, 2012, **24**, 2441-2446.
19. D. K. Hwang, C. Fuentes-Hernandez, J. D. Berrigan, Y. N. Fang, J. Kim, W. J. Potscavage, H. Cheun, K. H. Sandhage and B. Kippelen, *J. Mater. Chem.*, 2012, **22**, 5531-5537.
20. S. Hunter, J. H. Chen and T. D. Anthopoulos, *Adv. Funct. Mater.*, 2014, **24**, 5969-5976.
21. K. Zhao, O. Wodo, D. D. Ren, H. U. Khan, M. R. Niazi, H. L. Hu, M. Abdelsamie, R. P. Li, E. Q. Li, L. Y. Yu, B. Y. Yan, M. M. Payne, J. Smith, J. E. Anthony, T. D. Anthopoulos, S. T. Thoroddsen, B. Ganapathysubramanian and A. Amassian, *Adv. Funct. Mater.*, 2016, **26**, 1737-1746.
22. A. K. K. Kyaw, D. H. Wang, H. R. Tseng, J. Zhang, G. C. Bazan and A. J. Heeger, *Appl. Phys. Lett.*, 2013, **102**.
23. P. Sonar, E. L. Williams, S. P. Singh, S. Manzhos and A. Dodabalapur, *Phys. Chem. Chem. Phys.*, 2013, **15**, 17064-17069.
24. F. Garnier, G. Horowitz, X. Z. Peng and D. Fichou, *Synth. Met.*, 1991, **45**, 163-171.
25. G. Horowitz, X. Z. Peng, D. Fichou and F. Garnier, *J. Mol. Electron.*, 1991, **7**, 85-89.

26. A. Dodabalapur, L. Torsi and H. E. Katz, *Science*, 1995, **268**, 270-271.
27. H. E. Katz, L. Torsi and A. Dodabalapur, *Chem. Mater.*, 1995, **7**, 2235-2237.
28. T. Muck, V. Wagner, U. Bass, M. Leufgen, J. Geurts and L. W. Molenkamp, *Synth. Met.*, 2004, **146**, 317-320.
29. R. Singh, J. S. Meena, I. H. Tsai, Y. T. Lin, C. J. Wang and F. H. Ko, *Org. Electron.*, 2015, **19**, 120-130.
30. G. Horowitz, D. Fichou, X. Z. Peng, Z. G. Xu and F. Garnier, *Solid State Commun.*, 1989, **72**, 381-384.
31. F. Biscarini, R. Zamboni, P. Samorì, P. Ostoja and C. Taliani, *Phys. Rev. B*, 1995, **52**, 14868-14877.
32. P. Leclere, M. Surin, R. Lazzaroni, A. F. M. Kilbinger, O. Henze, P. Jonkheijm, F. Biscarini, M. Cavallini, W. J. Feast, E. W. Meijer and A. P. H. J. Schenning, *J. Mater. Chem.*, 2004, **14**, 1959-1963.
33. G. Barbarella, M. Melucci and G. Sotgiu, *Adv. Mater.*, 2005, **17**, 1581-1593.
34. F. Dinelli, R. Capelli, M. A. Loi, M. Murgia, M. Muccini, A. Facchetti and T. J. Marks, *Adv. Mater.*, 2006, **18**, 1416-1420.
35. S. Duhm, Q. Xin, N. Koch, N. Ueno and S. Kera, *Org. Electron.*, 2011, **12**, 903-910.
36. M. Ashizawa, T. Niimura, Y. Yu, K. Tsuboi, H. Matsumoto, R. Yamada, S. Kawauchi, A. Tanioka and T. Mori, *Tetrahedron*, 2012, **68**, 2790-2798.
37. D. V. Anokhin, M. Defaux, A. Mourran, M. Moeller, Y. N. Luponosov, O. V. Borshchev, A. V. Bakirov, M. A. Shcherbina, S. N. Chvalun, T. Meyer-Friedrichsen, A. Elschner, S. Kirchmeyer, S. A. Ponomarenko and D. A. Ivanov, *J. Phys. Chem. C*, 2012, **116**, 22727-22736.
38. G. Generali, F. Dinelli, R. Capelli, S. Toffanin, F. di Maria, M. Gazzano, G. Barbarella and M. Muccini, *J. Phys. Chem. C*, 2011, **115**, 23164-23169.
39. T. Leydecker, D. T. Duong, A. Salleo, E. Orgiu and P. Samorì, *ACS Appl. Mater. Inter.*, 2014, **6**, 21248-21255.
40. W. Y. Zhou, Y. G. Wen, L. C. Ma, Y. Q. Liu and X. W. Zhan, *Macromolecules*, 2012, **45**, 4115-4121.
41. P. Kohn, S. Huettner, H. Komber, V. Senkovskyy, R. Tkachov, A. Kiriy, R. H. Friend, U. Steiner, W. T. S. Huck, J. U. Sommer and M. Sommer, *J. Am. Chem. Soc.*, 2012, **134**, 4790-4805.
42. M. Anni, G. Gigli, V. Paladini, R. Cingolani, G. Barbarella, L. Favaretto, G. Sotgiu and M. Zambianchi, *Appl. Phys. Lett.*, 2000, **77**, 2458-2460.
43. M. Melucci, G. Barbarella, M. Zambianchi, P. Di Pietro and A. Bongini, *J. Org. Chem.*, 2004, **69**, 4821-4828.
44. O. Gidron, A. Dadvand, E. W. H. Sun, I. Chung, L. J. W. Shimon, M. Bendikov and D. F. Perepichka, *J. Mater. Chem. C*, 2013, **1**, 4358-4367.
45. D. H. Han and B. E. Park, *AIP Conf. Proc.*, 2011, **1399**.
46. E. M. Mannebach, J. W. Spalenka, P. S. Johnson, Z. H. Cai, F. J. Himpsel and P. G. Evans, *Adv. Funct. Mater.*, 2013, **23**, 554-564.
47. F. Dinelli, M. Murgia, P. Levy, M. Cavallini, F. Biscarini and D. M. de Leeuw, *Phys. Rev. Lett.*, 2004, **92**.
48. M. Kasha, H. R. Rawls and M. Ashraf El-Bayoumi, *Pure Appl. Chem.*, 1965, **11**, 371-392.
49. N. Winograd, *Surf. Interface Anal.*, 2013, **45**, 3-8.
50. A. Benninghoven, *Angew. Chem. Int. Edit.*, 1994, **33**, 1023-1043.
51. A. Facchetti, M. Mushrush, H. E. Katz and T. J. Marks, *Adv. Mater.*, 2003, **15**, 33-38.